Normal form for the onset of collapse: The prototypical example of the nonlinear Schrödinger equation

S. J. Chapman
Mathematical Institute, University of Oxford, AWB, ROQ, Woodstock Road, Oxford OX2 6GG, England

M. Kavousanakis
School of Chemical Engineering, National Technical University of Athens, 15780, Athens, Greece

I. G. Kevrekidis
Department of Chemical and Biomolecular Engineering and Department of Applied Mathematics and Statistics, Johns Hopkins University, Baltimore, Maryland 21218, USA

P. G. Kevrekidis
Department of Mathematics and Statistics, University of Massachusetts, Amherst, Massachusetts 01003-4515, USA and Mathematical Institute, University of Oxford, AWB, ROQ, Woodstock Road, Oxford OX2 6GG, England

(Received 17 August 2020; accepted 13 September 2021; published 4 October 2021)

The study of nonlinear waves that collapse in finite time is a theme of universal interest, e.g., within optical, atomic, plasma physics, and nonlinear dynamics. Here we revisit the quintessential example of the nonlinear Schrödinger equation and systematically derive a normal form for the emergence of radially symmetric blowup solutions from stationary ones. While this is an extensively studied problem, such a normal form, based on the methodology of asymptotics beyond all algebraic orders, applies to both the dimension-dependent and power-law-dependent bifurcations previously studied. It yields excellent agreement with numerics in both leading and higher-order effects, it is applicable to both infinite and finite domains, and it is valid in both critical and supercritical regimes.

DOI: 10.1103/PhysRevE.104.044202

I. INTRODUCTION

The nonlinear Schrödinger (NLS) model [1–4] is, arguably, one of the most central nonlinear partial differential equations (PDEs) within mathematical physics. NLS is a ubiquitous envelope wave equation for various physical contexts. Its applications span water waves [5–7], nonlinear optical media [8,9], plasma physics [10], and more recently, the atomic physics realm of Bose-Einstein condensates [11,12].

The solitary waves of NLS have been central to all of the above investigations. A similarly prominent feature of NLS is its finite-time, self-similar blowup in higher (integer) dimensions or for higher nonlinearity powers. Indeed, this has been central to both books [3,13,14] and reviews [15–17] and the object of continued study in the physical and mathematical literature; see, e.g., [18–20] and [21,22] for some recent examples and [23] for connections with Keller-Segel models of bacterial colonies. Importantly for our purposes, these focusing aspects have become accessible to physical experiments. In nonlinear optics, the well-known, two-dimensional collapsing wave form of the Townes soliton has been observed [24], as well as the collapse of optical vortices [25] or the loss of phase information of collapsing filaments [26]. Also, in the flourishing area of Bose-Einstein condensates, the Townes soliton has recently been announced [27], while collapsing wave forms in higher dimensions had been experimentally identified earlier [28,29].

The emergence of collapsing solutions out of solitonic ones has been long studied [30,31] and summarized in numerous reviews and books [3,13,14]. Nevertheless, remarkably, a normal form—a prototypical model equation compactly describing the relevant bifurcation, namely, the onset of collapsing solutions out of noncollapsing ones as a nonlinearity or dispersion parameter is varied—does not exist, to the best of our knowledge. Recent attempts to capture even the well-known log-log law of the critical case and its corrections [18] will confirm that. It is known that at the critical point at which collapse emerges, $\sigma d = 2$ (with $\sigma d < 2$ being subcritical and $\sigma d > 2$ supercritical), where σ is the nonlinearity exponent and d the spatial dimension, a symmetry enabling self-similar rescaling of the solution towards becoming singular at a finite time (the so-called pseudo-conformal invariance) arises; for details, see, e.g., pp. 35–37 of [3]. Beyond this critical point, solitary waves become unstable and, in a form somewhat reminiscent of the traditional pitchfork bifurcation, two collapsing branches of solutions emerge [32]. Yet, this is no ordinary pitchfork like, e.g., the one experimentally probed in BECs in double-well potentials [33]. Here, pseudoconformal symmetry breaks and, thus, collapse phenomena will not follow the standard cubic pitchfork normal form but rather are

associated with the exponentially small, beyond-all-algebraic-orders phenomenology of the relevant symmetry breaking. Our aim is to go beyond the heuristic (steady state only) arguments of earlier studies [30,31] and the rigorous, albeit qualitative, results in this direction of [34] and present a systematic quantitative derivation of the associated normal form. It is worth noting that while d is an integer parameter and σ is typically such that 2σ is integer in physical applications, here we will use these as continuous parameters in order to systematically unfold the relevant bifurcation structure of the system. Key features of our analysis are the following:

(1) We unify the case of general nonlinearity exponent and that of arbitrary dimension, offering a result *broadly applicable* in the above physical settings of interest.

(2) Our analysis captures both the case of the *critical* log-log collapse *and* the *supercritical* $t^{-1/2}$ *collapse*.

(3) Crucially, we capture not only the leading collapse order but also systematically the *higher-order corrections*.

(4) We find *excellent agreement* with computations of the stationary solutions and of the dynamical evolution. Despite the perturbative nature of the approach, analytical and numerical results remain nearly indistinguishable for a wide parametric range.

II. PROBLEM FORMULATION AND ASYMPTOTIC ANALYSIS

Our starting point is the radially symmetric NLS in dimension d with nonlinearity determined by the exponent σ:

$$i\frac{\partial\psi}{\partial t}+\frac{\partial^2\psi}{\partial r^2}+\frac{(d-1)}{r}\frac{\partial\psi}{\partial r}+|\psi|^{2\sigma}\psi=0. \tag{1}$$

For the self-similar dynamics of such *radially symmetric* models in the vicinity of the critical case $d\sigma=2$ [3,13], we establish the normal form of Eq. (21) below. While we will principally analyze the supercritical case of $d\sigma>2$, our formulation covers also the critical ($\sigma d=2$) and subcritical ($\sigma d<2$) cases. Our aim is to obtain the self-similar solution profile and, more importantly, the reduced, normal form dynamics of its rate of collapse (i.e., the rate of amplitude growth or of width shrinkage), assuming localized initial conditions subject to collapse. The consideration of sufficient conditions for collapse is an important problem that has been considered elsewhere [35,36]. Our consideration of radially symmetric data is justified, since nonisotropic initial conditions converge towards a radially symmetric profile, as was originally numerically observed in [37] and subsequently studied in [38,39].

Introducing the well-known stretched variables [3,13,32], involving the time-dependent width factor $L(t)$,

$$\xi=\frac{r}{L},\quad \tau=\int_0^t\frac{dt'}{L^2(t')},\quad \psi(r,t)=L^{-1/\sigma}e^{i\tau}v(\xi,\tau)$$

leads to

$$i\frac{\partial v}{\partial\tau}+\frac{\partial^2 v}{\partial\xi^2}+\frac{(d-1)}{\xi}\frac{\partial v}{\partial\xi}+|v|^{2\sigma}v-v+iG\left(\xi\frac{\partial v}{\partial\xi}+\frac{1}{\sigma}v\right)=0, \tag{2}$$

where the blowup rate is defined by

$$G=-LL_t=-L_\tau/L. \tag{3}$$

Notice that this suggests a shrinking solution width for $G>0$ and an expanding one for $G<0$. In this dynamic change of variables, and in order to close the dynamics in this "co-exploding" frame [upon determining $[G(\tau)]$, we impose a pinning condition of the form [32]

$$\int_{-\infty}^{\infty}\mathrm{Re}[v(\xi,\tau)]T(\xi)\,d\xi=C \tag{4}$$

for some constant C and some (essentially arbitrary) "template function" T, to enable us to uniquely identify the solution v and the blowup rate G. In our numerical examples we choose $T=\delta(\xi-2)$ [40]. Finally, we write

$$v(\xi,\tau)=V(\xi,\tau)e^{-iG(\tau)\xi^2/4}$$

to give (using $G'\equiv dG/d\tau$)

$$i\frac{\partial V}{\partial\tau}+\frac{G'\xi^2}{4}V+\frac{\partial^2 V}{\partial\xi^2}+\frac{(d-1)}{\xi}\frac{\partial V}{\partial\xi}+|V|^{2\sigma}V-V-\frac{i(d\sigma-2)G}{2\sigma}V+\frac{G^2\xi^2}{4}V=0. \tag{5}$$

For our time-dependent numerical results, Eq. (2) is spatially discretized using second-order central finite differences and integrated in time using MATLAB'S ode23t. To solve the steady-state problem we used CHEBFUN [41]. Asymptotically, we aim to solve (5) in the limit $G\to 0$ and $d\sigma\to 2$. Our strategy will be as follows. We will solve (5) separately in the near [$\xi=O(1)$] and far [$\xi=O(G^{-1})$] fields [42]. We will find that the far field has a *turning point* at $\xi G=2$, resulting in an exponentially small reflection back towards the near field [43]. Matching with the near-field solution yields our onset-of-collapse normal form.

A. Near field

We suppose (and will verify through our analysis) that the solution evolves exponentially slowly and that σ and d are exponentially close to σ_c, d_c satisfying $d_c\sigma_c=2$ [3,13]. Thus the second from the left and from the right terms in Eq. (5) can be neglected for now. We look for a solution:

$$V=e^{i\Phi(\tau)}[V_{\mathrm{reg}}(\xi,\tau;G(\tau))+V_{\mathrm{exp}}(\xi,\tau)], \tag{6}$$

where V_{reg} is the (real) regular algebraic expansion in G, V_{exp} is exponentially small in G, and the exponentially-slowly-varying phase Φ is determined by the pinning condition.

We expand the solution in (even and odd) powers of G (with $G>0$) as

$$V_{\mathrm{reg}}=\sum_{n=0}^{\infty}G^{2n}V_n,\quad \Phi=\sum_{n=0}^{\infty}G^{2n+1}\Phi_n. \tag{7}$$

That the expansion for V contains only even powers of G follows from the correction term in Eq. (5) being proportional to G^2; that the expansion for Φ contains only odd powers of G follows from the pinning condition—see Eq. (37) below. This gives the leading-order equation

$$\frac{\partial^2 V_0}{\partial\xi^2}+\frac{(d_c-1)}{\xi}\frac{\partial V_0}{\partial\xi}+V_0^{2\sigma_c+1}-V_0=0, \tag{8}$$

the solution of which is the critical ground-state soliton. The next order V_1 then satisfies

$$\frac{\partial^2 V_1}{\partial \xi^2} + \frac{(d_c-1)}{\xi}\frac{\partial V_1}{\partial \xi} + \left(\frac{4}{d_c}+1\right)V_0^{2\sigma_c}V_1 - V_1 = -\frac{\xi^2 V_0}{4}, \tag{9}$$

with $V_1'(0) = 0$, and $V_1 \to 0$ as $\xi \to \infty$.

B. Far field

The expansion (7) breaks down at large distances, when $V_{\rm reg}$ is small. For small amplitudes the $|V_{\rm reg}|^{2\sigma}V_{\rm reg}$ term is negligible, and a linear analysis of the corresponding operator shows that $V_{\rm reg}$ decays exponentially. Similarly, as $\xi \to \infty$, the solution to (8) is dominated by

$$V_0(\xi) \sim \frac{A_{d_c}e^{-\xi}}{\xi^{(d_c-1)/2}} = \frac{A_{d_c}G^{(d_c-1)/2}e^{-\rho/G}}{\rho^{(d_c-1)/2}}, \tag{10}$$

for some dimension-dependent constant A_{d_c}. We note, in particular, the values $A_1 = 12^{1/4}$ (from the quintic NLS exact soliton solution [3]), and $A_2 \approx 3.518$ [18].

In the far field we rescale $\xi = \rho/G$ to give

$$G^2\frac{\partial^2 V_{\rm reg}}{\partial \rho^2} + G^2\frac{(d_c-1)}{\rho}\frac{\partial V_{\rm reg}}{\partial \rho} + |V_{\rm reg}|^{2\sigma_c}V_{\rm reg} - V_{\rm reg} + \frac{\rho^2}{4}V_{\rm reg} = 0.$$

The exponential decay of $V_{\rm reg}$ renders it exponentially small in G in the far field, allowing us to neglect the nonlinear term $|V_{\rm reg}|^{2\sigma_c}V_{\rm reg}$. We now look for a WKB solution as

$$V_{\rm reg} \sim G^k e^{\phi(\rho)/G}\sum_{n=0}^{\infty} A_n(\rho)G^n, \tag{11}$$

with k to be determined below. At leading order this gives the following eikonal equation:

$$(\phi')^2 = 1 - \frac{\rho^2}{4} \quad \Rightarrow \quad \phi = -\int_0^\rho \left(1-\frac{\bar\rho^2}{4}\right)^{1/2} d\bar\rho \tag{12}$$

(so that $V_{\rm reg}$ is decreasing in ρ). Note the turning point at $\rho = 2$ from Eq. (12). The amplitude equation for A_0 then leads to

$$A_0 = \frac{a_0}{\rho^{(d_c-1)/2}(-\phi')^{1/2}} = \frac{2^{1/2}\,a_0}{\rho^{(d_c-1)/2}(4-\rho^2)^{1/4}},$$

for some constant a_0, which we will determine by matching with the near-field solution (10). As $\rho \to 0$, the far field yields

$$G^k e^{\phi(\rho)/G}A_0 \sim \frac{a_0 G^k e^{-\rho/G}}{\rho^{(d_c-1)/2}}. \tag{13}$$

Matching (13) with (10) gives $k = (d_c-1)/2$ and $a_0 = A_{d_c}$.

For $\rho > 2$ only the solution of (12) in which

$$\phi' = i\left(\frac{\rho^2}{4}-1\right)^{1/2}$$

has a finite Hamiltonian. Thus for $\rho > 2$,

$$V_{\rm reg} = \alpha G^k e^{i\phi_2(\rho)/G}\sum_{n=0}^{\infty} B_n(\rho)(iG)^n, \tag{14}$$

for some constant α, where

$$\phi_2 = \int_2^\rho \left(\frac{\bar\rho^2}{4}-1\right)^{1/2} d\bar\rho, \quad B_0(\rho) = \frac{2^{1/2}a_0}{\rho^{(d_c-1)/2}(\rho^2-4)^{1/4}}.$$

The fact that only one of the oscillatory exponentials arises beyond the turning point, i.e., for $\rho > 2$, forces an *exponentially small reflection* back towards the near field, which we will obtain by analyzing the turning point region. This is a key feature of our exponential asymptotics analysis.

C. Turning point

We see that $A_0, B_0 \to \infty$ as $\rho \to 2$ corresponding to the WKB approximation breaking down as the turning point is approached, requiring an "inner" analysis in its vicinity. To approximate the solution in the vicinity of the turning point we rescale the independent variable as $\rho = 2 + G^{2/3}s$. Then, with $s = O(1)$ as $G \to 0$, the equation near the turning point becomes, to leading order,

$$\frac{d^2 V_{\rm reg}}{ds^2} + sV_{\rm reg} = 0,$$

with the solution $V_{\rm reg} = \lambda{\rm Ai}(-s) + \mu{\rm Bi}(-s)$, where Ai and Bi are Airy functions of the first and second kind, respectively. The asymptotic expansions of Ai and Bi give

$$V_{\rm reg} \sim \frac{\lambda e^{-2(-s)^{3/2}/3}}{2\sqrt{\pi}(-s)^{1/4}} + \frac{\mu e^{2(-s)^{3/2}/3}}{\sqrt{\pi}(-s)^{1/4}} \quad \text{as } s \to -\infty, \tag{15}$$

$$V_{\rm reg} \sim \frac{e^{2is^{3/2}/3}}{2\sqrt{\pi}s^{1/4}}(\lambda e^{-i\pi/4} + \mu e^{i\pi/4}) + \frac{e^{-2is^{3/2}/3}}{2\sqrt{\pi}s^{1/4}}(\lambda e^{i\pi/4} + \mu e^{-i\pi/4}) \quad \text{as } s \to \infty. \tag{16}$$

Matching with (11) and (14) gives $\alpha = e^{i\pi/4}$ and

$$\lambda = i\mu = a_0 i\sqrt{\pi}G^{k-1/6}e^{\phi(2)/G}.$$

Including both WKB solutions in $\rho < 2$ replaces (11) with

$$V_{\rm reg} \sim (e^{\phi(\rho)/G} + \gamma e^{-\phi(\rho)/G})G^k\sum_{n=0}^{\infty} A_n(\rho)G^n, \tag{17}$$

where matching with (15) gives

$$\gamma = \frac{i}{2}e^{2\phi(2)/G} = \frac{i}{2}e^{-\pi/G}.$$

D. Exponentially small correction to the near field

As $\rho \to 0$, using Eq. (13), we have

$$\gamma e^{-\phi(\rho)/G}G^k\sum_{n=0}^{\infty} A_n(\rho)G^n \sim \frac{a_0\gamma G^{(d_c-1)/2}e^{\rho/G}}{\rho^{(d_c-1)/2}}. \tag{18}$$

This term will match with the exponentially small correction to the near field. In the original near-field scaling, using Eq. (6) neglecting time derivatives and quadratic terms in $V_{\rm exp}$ (which are doubly exponentially small), but keeping all the other

exponentially small terms, gives

$$\frac{\partial^2 V_{\rm exp}}{\partial \xi^2} + \frac{(d_c-1)}{\xi}\frac{\partial V_{\rm exp}}{\partial \xi} + V_{\rm reg}^{2\sigma_c}[\sigma_c V_{\rm exp}^* + (\sigma_c+1)V_{\rm exp}] - V_{\rm exp} + \frac{G^2\xi^2}{4}V_{\rm exp} = -\frac{(d-d_c)}{\xi}\frac{\partial V_{\rm reg}}{\partial \xi} - i\frac{\partial V_{\rm reg}}{\partial \tau} + \Phi' V_{\rm reg} - \frac{G'\xi^2}{4}V_{\rm reg} - 2(\sigma-\sigma_c)V_{\rm reg}^{2\sigma_c+1}\log V_{\rm reg} + \frac{i(d\sigma-2)G}{2\sigma}V_{\rm reg},$$

where $\Phi' = d\Phi/d\tau$. We now use $V_{\rm exp} = U_{\rm exp} + iW_{\rm exp}$ and separate into real and imaginary parts. Since $V_{\rm reg}$ satisfies the homogeneous version of the equation for $W_{\rm exp}$, there is a solvability condition: multiplying that equation by $\xi^{d_c-1}V_{\rm reg}$, integrating from 0 to R, and using (8), we obtain

$$R^{d_c-1}V_{\rm reg}(R)\frac{\partial W_{\rm exp}}{\partial \xi}(R) - R^{d_c-1}W_{\rm exp}(R)\frac{\partial V_{\rm reg}}{\partial \xi}(R) = -\int_0^R \xi^{d_c-1}V_{\rm reg}\frac{\partial V_{\rm reg}}{\partial \tau} - \xi^{d_c-1}\frac{(d\sigma-2)G}{2\sigma}V_{\rm reg}^2\,d\xi. \tag{19}$$

As $R\to\infty$ we evaluate the boundary terms by matching using (18), giving

$$\lim_{R\to\infty} R^{d_c-1}\left(V_{\rm reg}(R)\frac{\partial W_{\rm exp}}{\partial \xi}(R) - W_{\rm exp}(R)\frac{\partial V_{\rm reg}}{\partial \xi}(R)\right) \sim \lim_{R\to\infty} a_0 e^{-R}(a_0{\rm Im}(\gamma)e^R) - (a_0{\rm Im}(\gamma)e^R)(-a_0e^{-R}) = 2a_0^2{\rm Im}(\gamma).$$

Now

$$\int_0^\infty \xi^{d_c-1}V_{\rm reg}^2\,d\xi \sim \int_0^\infty \xi^{d_c-1}(V_0+G^2V_1+\cdots)^2\,d\xi \sim b_0 + 2G^2c_0 + \cdots,$$

say, where

$$b_0 = \int_0^\infty \xi^{d_c-1}V_0^2\,d\xi, \quad c_0 = \int_0^\infty \xi^{d_c-1}V_0V_1\,d\xi.$$

Thus the solvability condition (19) gives

$$2c_0G\frac{dG}{d\tau} = \frac{(d\sigma-2)b_0}{2\sigma}G - A_{d_c}^2 e^{-\pi/G}. \tag{20}$$

A similar analysis can be performed when $G<0$. Combining the two results gives

$$2c_0G\frac{dG}{d\tau} = \frac{(d\sigma-2)}{2\sigma}b_0G - A_{d_c}^2\,{\rm sgn}(G)\,e^{-\pi/|G|}, \tag{21}$$

which is our principal result, namely, the *normal form for the onset of collapse*. We note that the normal form preserves the symmetry $\tau\to-\tau$, $G\to-G$ [and $V\to V^*$] of (5).

The natural bifurcation parameter is $r=(d\sigma-2)$. For all $r<0$, $G=0$ is the only equilibrium branch of solutions. When $r>0$ this branch becomes unstable, and two new nontrivial equilibrium branches emerge. In contrast to the usual pitchfork bifurcation, here the branch with $G>0$ is stable (corresponding to a stable collapse in forward time) while the branch with $G<0$ is unstable (corresponding to stably collapsing in negative time, i.e., "coming back from infinity"). Moreover, a key feature here is the exponential (rather than the standard power law) nature of the bifurcation of the collapsing branch, yielding a nearly vertical bifurcation for $G=G(\sigma)$, as shown in Fig. 1.

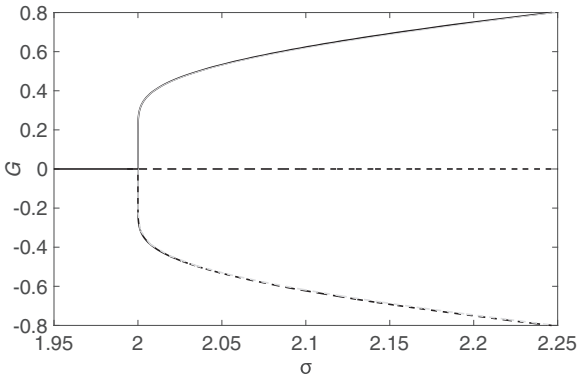

FIG. 1. Variation of the blowup rate G of Eq. (3), as a function of σ for $d=1$, domain size $K=50$. PDE results (black lines) obtained from Eq. (2) are in excellent agreement with the asymptotic solution obtained from Eq. (23) [with a and b truncated at $O(G^2)$, gray lines]. The solitonic branch ($G=0$) is stable up to $\sigma=2$ (solid line) and becomes unstable for $\sigma>2$ (dashed line). The stable collapsing branch ($G>0$) is depicted with solid line, and the mirror image [i.e., arising for $G\to-G$, $\tau\to-\tau$ and ${\rm Im}(v)\to-{\rm Im}(v)$] branch in the bottom ($G<0$) is illustrated with dash-dotted line.

Before we compare with direct numerical simulations, we extend our analysis both by calculating higher-order terms in the normal form (21) and by considering the effect of a finite domain. First, though, we illustrate the relationship between (20) and the well-known log log law of collapse.

E. The log - log law of collapse

Notice that our analysis is still valid for $r=0$. We show that in this case the asymptotic behavior of (20) as $\tau\to\infty$ implies the well-known log-log law of collapse.

In the critical case, with $G>0$, Eq. (20) is

$$2c_0G\frac{dG}{d\tau} = -A_d^2e^{-\pi/G}. \tag{22}$$

Recall

$$\frac{d\tau}{dz} = \frac{1}{L^2}, \quad G(\tau) = -LL_z = -\frac{L_\tau}{L}.$$

Integrating this last equation,

$$\log\frac{L}{L(0)} = -\int_0^\tau G(\tau)\,d\tau = \frac{2c_0}{A_d^2}\int_{G(0)}^G \tilde{G}^2e^{\pi/\tilde{G}}\,d\tilde{G} \sim -\frac{2c_0}{A_d^2\pi}G^4e^{\pi/G},$$

as $\tau\to\infty$ and $G\to0$. Thus, at leading order (which is what is needed for the log - log law)

$$G\sim\frac{\pi}{\log(-\log L)}.$$

Then,

$$z_c - z(\tau) = \int_\tau^\infty L^2\, d\tau = \int_0^L \frac{\tilde{L}}{G(\tilde{L})}\, d\tilde{L} \sim \int_0^L \frac{\tilde{L}\log\log 1/\tilde{L}}{\pi}\, dL \sim \frac{L^2 \log\log 1/L}{2\pi}$$

as $L \to 0$. Thus

$$L^2 \sim \frac{2\pi(z_c - z)}{\log\log 1/L} \sim \frac{2\pi(z_c - z)}{\log|\log(z_c - z)|}$$

as expected. However, as noted in [18], this leading-order asymptotic behavior of L as $z \to z_c$ is so weak that it requires unrealistically large amplitudes before it is observed. This is associated with the fact that $G(\tau) \to 0$ only logarithmically as $\tau \to \infty$, so that the leading-order asymptotics of Eq. (22) for large τ is only a good approximation at very large τ. However, Eq. (22) itself (in contrast to its large τ asymptotics) provides a good approximation to $G(\tau)$ for all τ (except possibly for an initial $\tau = O(1)$ transient, as is discussed in our numerical implementation within Sec. II I).

F. Higher-order terms

While Eq. (21) includes only the leading-order behavior of each term, higher-order corrections can be calculated in a systematic manner. Higher-order terms in the evaluation of the right-hand side of (19) are straightforward to evaluate, requiring simply the evaluation of more terms in the regular expansion (7). Evaluating higher-order terms in the left-hand side of (19) is more challenging but still possible. The result is

$$2c(G)G\frac{dG}{d\tau} = \frac{(d\sigma - 2)}{2\sigma} b(G)G - a(G)^2 \mathrm{sgn}(G) e^{-\pi/|G|}, \tag{23}$$

where a, b, and c have power series expansions in G^2. In some of our numerical examples we include the $O(G^2)$ and $O(G^4)$ terms in the expansions of a, b, and c. To simplify the presentation, we illustrate the calculation for the case $d = 1$, with $G > 0$.

We write the dominant WKB solution in the far field as

$$V_{\mathrm{reg}} \sim \kappa(G) G^k e^{\phi(\rho)/G} \sum_{n=0}^{\infty} A_n(\rho) G^n, \tag{24}$$

where $\kappa \sim 1$ as $G \to 0$. Most of the difficulty in determining the higher-order terms in (23) comes from the problem of determining κ, which we defer to Secs. II F 1 and II F 2 below.

Once we know κ, the turning point calculation is essentially unchanged and gives simply the amplitude of the exponentially small reflected field as $\kappa\gamma$. The solvability condition (19) then gives

$$\frac{1}{2}\int_0^\infty \frac{\partial V_{\mathrm{reg}}^2}{\partial \tau}\, d\xi - \frac{(d\sigma - 2)}{2\sigma} G \int_0^\infty V_{\mathrm{reg}}^2\, d\xi = -2a_0^2\kappa^2 \mathrm{Im}(\gamma), \tag{25}$$

where for an infinite domain $\mathrm{Im}(\gamma) = e^{-\pi/G}/2$ (while for a finite domain γ is given by (33), as is elaborated below). Substituting in the expansion (7) for V_{reg} gives an asymptotic series for each term on the left-hand side. In particular, if we write

$$\int_0^\infty \frac{\partial V_{\mathrm{reg}}^2}{\partial \tau}\, d\xi = 4cG\frac{\partial G}{\partial \tau}, \quad \int_0^\infty V_{\mathrm{reg}}^2\, d\xi = b,$$

then

$$2c\frac{\partial G}{\partial \tau} = \frac{(d\sigma - 2)}{2\sigma} b - 2a_0^2\kappa^2 \mathrm{Im}(\gamma),$$

with

$$b \sim \frac{\sqrt{3}\,\pi}{4} + \frac{\sqrt{3}\,\pi^3}{256} G^2 + 0.380\, G^4 + \cdots,$$

$$c \sim \frac{\sqrt{3}\,\pi^3}{512} + 0.380\, G^2 + 2.016\, G^4 + \cdots.$$

The expansion for κ, determined below, is

$$\kappa(G) \sim 1 - \left(\frac{1 + 12\pi^2}{4608}\right) G^2 + 0.0152\, G^4 + \cdots.$$

To show this we need to match the higher-order terms in the far-field expansion (24) with the near-field solution.

1. Higher-order terms in the far field

Let us return to the far-field expression (24). The equation for A_1 is

$$2A_1'\phi' + A_0'' + A_1\phi'' = 0,$$

i.e.,

$$\frac{d}{d\rho}[A_1(-\phi')^{1/2}] = \frac{A_0''}{2(-\phi')^{1/2}} = \frac{a_0(8 + 3\rho^2)}{4(4 - \rho^2)^{5/2}}.$$

Thus,

$$A_1 = \frac{a_0\rho(24 - \rho^2)}{24\sqrt{2}\,(4 - \rho^2)^{7/4}},$$

where the arbitrary multiple of $(-\phi')^{-1/2}$ is proportional to A_0 and is absorbed into the coefficient $\kappa(G)$. Proceeding similarly at higher orders gives

$$A_2 = \frac{a_0(2320 - 996\rho^2 + 9\rho^4)}{576\sqrt{2}\,(4 - \rho^2)^{13/4}}, \quad A_3 = \frac{a_0\rho(33\,189\,120 + 4\,863\,840\rho^2 + 226\,296\rho^4 - 36\,378\rho^6 + 2021\rho^8)}{829\,440\sqrt{2}(4 - \rho^2)^{19/4}},$$

$$A_4 = \frac{a_0(3\,269\,916\,928 + 7\,846\,589\,568\rho^2 + 815\,011\,440\rho^4 - 619\,928\rho^6 - 321\,339\rho^8 + 18\,189\rho^{10})}{19\,906\,560\sqrt{2}(4 - \rho^2)^{25/4}}.$$

As $\rho \to 0$,

$$A_0 \to a_0, \quad A_1 \to 0, \quad A_2 \to \frac{145a_0}{4608}, \quad A_3 \to 0, \quad A_4 \to \frac{12\,773\,113a_0}{637\,009\,920}.$$

To determine higher-order terms in the expansion of κ, we need to match this behavior with the large-ξ behavior of the near-field solution.

2. Higher-order terms in outer limit of the inner expansion

When $d = 1$ we may solve (9) for V_1 using variation of parameters to give

$$V_1(\xi) = \frac{v_1(\xi)}{16}\int_0^\xi v_2(\bar\xi)\bar\xi^2 V_0(\bar\xi)\,d\bar\xi + \frac{v_2(\xi)}{16}\int_\xi^\infty v_1(\bar\xi)\bar\xi^2 V_0(\bar\xi)\,d\bar\xi, \tag{26}$$

where

$$v_1 = \frac{\sinh(2\xi)}{\cosh^{3/2}(2\xi)}, \quad v_2 = \frac{\cosh(4\xi)-3}{\cosh^{3/2}(2\xi)}.$$

As $\xi \to \infty$,

$$v_1 \sim 2^{1/2}e^{-\xi}, \quad v_2 \sim 2^{1/2}e^{\xi}, \quad V_0 \sim 12^{1/4}e^{-\xi},$$

and therefore we obtain

$$\begin{aligned} V_1 &\sim \frac{\sqrt2}{16}\int_0^\infty (v_2\bar\xi^2 V_0 - 12^{1/4}2^{1/2}\bar\xi^2)\,d\bar\xi + \frac{\sqrt2}{16}\int_0^\xi 12^{1/4}2^{1/2}\bar\xi^2\,d\bar\xi + \frac{\sqrt2}{16}\int_\xi^\infty 2^{1/2}12^{1/4}\bar\xi^2 e^{-2\bar\xi}\,d\bar\xi \\ &= \left(-\frac{\pi^2}{64\sqrt2\,3^{3/4}} + \frac{\xi^3}{4\sqrt2\,3^{3/4}} + \frac{3^{1/4}}{16\sqrt2}(1+2\xi+2\xi^2)\right)e^{-\xi} \\ &= (\omega_0+\omega_1\xi+\omega_2\xi^2+\omega_3\xi^3)e^{-\xi}, \end{aligned}$$

defining in this way the ω_i's. The crucial term which determines κ is the constant multiple of $e^{-\xi}$ at infinity, which is

$$\omega_0 = \frac{12-\pi^2}{64\sqrt2\,3^{3/4}}.$$

Before we do the matching, we do a similar calculation on V_2. If we write the general equation for V_n as

$$\mathcal{L}V_n = \mathrm{rhs}_n,$$

where $\mathcal{L}$ is the operator on the left-hand side of (9), then the solution is

$$\begin{aligned} V_n(\xi) = &-\frac{v_1(\xi)}{4}\int_0^\xi v_2(\bar\xi)\mathrm{rhs}_n(\bar\xi)\,d\bar\xi \\ &- v_2(\xi)\int_\xi^\infty \frac{v_1(\bar\xi)\mathrm{rhs}_n(\bar\xi)\,d\bar\xi}{4}. \end{aligned}$$

Now, for V_2,

$$\mathrm{rhs}_2 = -\frac{\xi^2 V_1}{4} - 10V_0^3V_1^2. \tag{27}$$

Again we are looking for the constant$\times e^{-\xi}$ term in V_2 as $\xi \to \infty$. The second term in (27) produces a constant$\times e^{-\xi}$ term in V_2 of

$$\frac{5\sqrt2}{2}e^{-\xi}\int_0^\infty v_2\bar\xi^2V_0^3V_1^2\,d\bar\xi \approx 0.039\,87e^{-\xi}.$$

The first term produces a constant$\times e^{-\xi}$ term of

$$\begin{aligned} &\frac{e^{-\xi}\sqrt2}{16}\int_0^\infty [v_2\bar\xi^2V_1 - 2^{1/2}\bar\xi^2(\omega_0+\omega_1\bar\xi+\omega_2\bar\xi^2+\omega_3\bar\xi^3)]\,d\bar\xi \\ &\quad + \frac{e^{-\xi}\sqrt2}{16}\int_0^\infty 2^{1/2}\bar\xi^2(\omega_0+\omega_1\bar\xi+\omega_2\bar\xi^2+\omega_3\bar\xi^3)e^{-2\bar\xi}\,d\bar\xi \\ &\quad \approx 0.024\,225e^{-\xi}. \end{aligned}$$

Putting the two contributions together, we find the constant$\times e^{-\xi}$ term in V_2 is

$$0.0641e^{-\xi}.$$

Matching the near field with the far field, recalling that $a_0 = 12^{1/4}$, now gives

$$\begin{aligned} &12^{1/4} + G^2\left(\frac{12-\pi^2}{64\sqrt2\,3^{3/4}}\right) + 0.0641G^4 + \cdots \\ &\quad = 12^{1/4}\kappa(G)\left(1 + \frac{145}{4608}G^2 + \frac{12\,773\,113}{637\,009\,920}G^4 + \cdots\right), \end{aligned}$$

so that

$$\kappa(G) \sim 1 - \left(\frac{1+12\pi^2}{4608}\right)G^2 + 0.0152\,G^4 + \cdots. \tag{28}$$

G. Finite domain

Usually, when numerically simulating (1) or (5) the domain is truncated to some large but finite domain $[0, K]$. In the critical case $d\sigma = 2$, this was earlier studied in [44,45]. For a finite domain both oscillatory WKB solutions are present in $\rho > 2$, and the ratio of their amplitudes is determined by the position of the boundary and the nature of the boundary condition. Here we impose the Neumann condition

$$\frac{\partial v}{\partial \xi} = 0 \quad \text{at } \xi = K. \tag{29}$$

We present the analysis for $G > 0$; a similar calculation may be performed when $G < 0$.

1. Far field beyond the turning point

In the far-field scaling $\xi = \rho/G$, Eq. (29) becomes

$$G\frac{\partial V}{\partial \rho} = \frac{i\rho V}{2} \quad \text{at } \rho = KG. \tag{30}$$

We see immediately that the turning point lies inside the domain only if $K > 2/G$. Let us first suppose that this is the case. Now both oscillatory exponentials are present for $\rho > 2$ and we have

$$V_{\text{reg}} = \alpha(G)G^k e^{i\phi_2(\rho)/G}\sum_{n=0}^{\infty} B_n(\rho)(iG)^n + \beta(G)G^k e^{-i\phi_2(\rho)/G}\sum_{n=0}^{\infty} B_n(\rho)(-iG)^n,$$

for some constants $\alpha(G)$, $\beta(G)$, where

$$\phi_2 = \int_2^{\rho}\left(\frac{\bar{\rho}^2}{4} - 1\right)^{1/2} d\bar{\rho}.$$

Then,

$$\begin{aligned}\frac{\partial V_{\text{reg}}}{\partial \rho} = {} & \frac{\alpha i\phi_2'(\rho)}{G}e^{i\phi_2(\rho)/G}G^k\sum_{n=0}^{\infty} B_n(\rho)(iG)^n + \alpha e^{i\phi_2(\rho)/G}G^k\sum_{n=0}^{\infty} B_n'(\rho)(iG)^n \\ & - \frac{\beta i\phi_2'(\rho)}{G}e^{-i\phi_2(\rho)/G}G^k\sum_{n=0}^{\infty} B_n(\rho)(-iG)^n + \beta e^{-i\phi_2(\rho)/G}G^k\sum_{n=0}^{\infty} B_n'(\rho)(-iG)^n.\end{aligned}$$

The boundary condition (30) accordingly gives

$$\begin{aligned}& \alpha i\phi_2'(KG)e^{i\phi_2(KG)/G}\sum_{n=0}^{\infty} B_n(KG)(iG)^n + \alpha G e^{i\phi_2(KG)/G}\sum_{n=0}^{\infty} B_n'(KG)(iG)^n \\ & \quad - \beta i\phi_2'(KG)e^{-i\phi_2(KG)/G}\sum_{n=0}^{\infty} B_n(KG)(-iG)^n + \beta G e^{-i\phi_2(KG)/G}\sum_{n=0}^{\infty} B_n'(KG)(-iG)^n \\ & = \frac{iKG}{2}\left(\alpha e^{i\phi_2(KG)/G}\sum_{n=0}^{\infty} B_n(KG)(iG)^n + \beta e^{-i\phi_2(KG)/G}\sum_{n=0}^{\infty} B_n(KG)(-iG)^n\right).\end{aligned}$$

Thus

$$\begin{aligned}& \alpha e^{i\phi_2(KG)/G}\left((2\phi_2'(KG) - KG)\sum_{n=0}^{\infty} B_n(KG)(iG)^n - 2iG\sum_{n=0}^{\infty} B_n'(KG)(iG)^n\right) \\ & = \beta e^{-i\phi_2(KG)/G}\left((2\phi_2'(KG) + KG)\sum_{n=0}^{\infty} B_n(KG)(-iG)^n + 2iG\sum_{n=0}^{\infty} B_n'(KG)(-iG)^n\right)\end{aligned}$$

so that

$$\beta = \nu\alpha e^{2i\phi_2(KG)/G}, \tag{31}$$

where

$$\nu = \frac{(2\phi_2'(KG) - KG)\sum_{n=0}^{\infty} B_n(KG)(iG)^n - 2iG\sum_{n=0}^{\infty} B_n'(KG)(iG)^n}{(2\phi_2'(KG) + KG)\sum_{n=0}^{\infty} B_n(KG)(-iG)^n + 2iG\sum_{n=0}^{\infty} B_n'(KG)(-iG)^n}.$$

This replaces the condition $\beta = 0$ which was imposed on an infinite domain. Assuming $KG = O(1)$, we obtain to leading order that

$$\nu \sim \nu_0 = \frac{\sqrt{(KG)^2 - 4} - KG}{\sqrt{(KG)^2 - 4} + KG}. \tag{32}$$

We see that $\nu_0 \to 0$ as $K \to \infty$ as expected.

2. Turning point

We now have

$$V_{\rm reg} = \alpha G^k e^{i\phi_2(\rho)/G} \sum_{n=0}^{\infty} B_n(\rho)(iG)^n + \beta G^k e^{-i\phi_2(\rho)/G} \sum_{n=0}^{\infty} B_n(\rho)(-iG)^n \quad \rho > 2,$$

$$V_{\rm reg} = G^k e^{\phi(\rho)/G} \sum_{n=0}^{\infty} A_n(\rho) G^n + \gamma G^k e^{-\phi(\rho)/G} \sum_{n=0}^{\infty} A_n(\rho)(-G)^n \quad \rho < 2,$$

where $\gamma(G)$ is the coefficient of the exponentially small reflection that we need to determine. Locally, with $\rho = 2 + G^{2/3}s$,

$$V_{\rm reg} \sim \frac{\alpha a_0}{G^{1/6-k}s^{1/4}} e^{2is^{3/2}/3} + \frac{\beta a_0}{G^{1/6-k}s^{1/4}} e^{-2is^{3/2}/3} \quad s > 0,$$

$$V_{\rm reg} \sim \frac{a_0}{G^{1/6-k}(-s)^{1/4}} e^{\phi(2)/G} e^{2(-s)^{3/2}/3} + \frac{\gamma a_0}{G^{1/6-k}(-s)^{1/4}} e^{-\phi(2)/G} e^{-2(-s)^{3/2}/3} \quad s < 0.$$

The equation near the turning point is still, at leading order,

$$\frac{d^2 V_{\rm reg}}{ds^2} + sV_{\rm reg} = 0,$$

with the solution

$$V_{\rm reg} = a_0\sqrt{\pi} G^{k-1/6}[\lambda {\rm Ai}(-s) + \mu {\rm Bi}(-s)],$$

and asymptotic behavior

$$V_{\rm reg} \sim \frac{\lambda a_0}{2G^{1/6-k}(-s)^{1/4}} e^{-2(-s)^{3/2}/3} + \frac{\mu a_0}{G^{1/6-k}(-s)^{1/4}} e^{2(-s)^{3/2}/3} \quad \text{as } s \to -\infty,$$

$$V_{\rm reg} \sim \frac{\lambda a_0}{G^{1/6-k}s^{1/4}} \frac{1}{2}\left(e^{2is^{3/2}/3 - i\pi/4} + e^{-2is^{3/2}/3 + i\pi/4}\right) + \frac{\mu a_0}{G^{1/6-k}s^{1/4}} \frac{1}{2i}\left(e^{-2is^{3/2}/3 + i\pi/4} - e^{2is^{3/2}/3 - i\pi/4}\right) \quad \text{as } s \to \infty,$$

leading this time to the connection formulas

$$\frac{\lambda}{2} = \gamma e^{-\phi(2)/G}, \quad \frac{\lambda e^{-i\pi/4}}{2} + \frac{\mu e^{i\pi/4}}{2} = \alpha, \quad \mu = e^{\phi(2)/G}, \quad \frac{\lambda e^{i\pi/4}}{2} + \frac{\mu e^{-i\pi/4}}{2} = \beta.$$

Eliminating λ and μ gives

$$e^{\phi(2)/G} = \alpha e^{-i\pi/4} + \beta e^{i\pi/4}, \quad 2\gamma e^{-\phi(2)/G} = \alpha e^{i\pi/4} + \beta e^{-i\pi/4}.$$

Now imposing (31) gives

$$\alpha = \frac{e^{i\pi/4} e^{\phi(2)/G}}{1 + i\nu e^{2i\phi_2(KG)/G}}$$

so that

$$\gamma = \frac{i}{2} e^{2\phi(2)/G} \left(\frac{1 - i\nu e^{2i\phi_2(KG)/G}}{1 + i\nu e^{2i\phi_2(KG)/G}}\right). \tag{33}$$

3. Exponentially small correction to the near field

Matching with the near field proceeds as in the case of an infinite domain, leading as before to

$$-2c_0 G \frac{dG}{d\tau} + \frac{(d\sigma - 2)G}{2\sigma} b_0 = 2a_0^2 {\rm Im}(\gamma). \tag{34}$$

At leading order ν is real and therefore

$${\rm Im}(\gamma) \sim \frac{(1 - \nu_0^2)e^{-\pi/G}}{2\left[1 - 2\nu_0 \sin\left(2\phi_2(KG)/G\right) + \nu_0^2\right]}, \tag{35}$$

where

$$\phi_2 = \int_2^{KG} \left(\frac{\bar{\rho}^2}{4} - 1\right)^{1/2} d\bar{\rho} = \frac{KG\sqrt{(KG)^2 - 4}}{4} - \log\left(\frac{KG + \sqrt{(KG)^2 - 4}}{2}\right),$$

and ν_0 is given by (32). We see that as $K \to \infty$, $\nu_0 \to 0$ and ${\rm Im}(\gamma) \to e^{-\pi/G}/2$, as expected.

4. Turning point outside the domain

For completeness we consider also the case in which $KG < 2$. Then the boundary condition (30) must be imposed directly on the far-field solution,

$$V_{\rm reg} \sim e^{\phi(\rho)/G}\sum_{n=0}^{\infty} A_n(\rho)G^n + \gamma e^{-\phi(\rho)/G}\sum_{n=0}^{\infty} A_n(\rho)(-G)^n,$$

giving

$$\phi'(KG)e^{\phi(KG)/G}\sum_{n=0}^{\infty} A_n(KG)G^n + Ge^{\phi(KG)/G}\sum_{n=0}^{\infty} A_n'(KG)G^n - \gamma\phi'(KG)e^{-\phi(KG)/G}\sum_{n=0}^{\infty} A_n(KG)(-G)^n$$
$$+ \gamma Ge^{-\phi(KG)/G}\sum_{n=0}^{\infty} A_n'(KG)(-G)^n = \frac{iKG}{2}\left(e^{\phi(KG)/G}\sum_{n=0}^{\infty} A_n(KG)G^n + \gamma e^{-\phi(KG)/G}\sum_{n=0}^{\infty} A_n(KG)(-G)^n\right).$$

At leading order

$$\gamma = \frac{2\phi'(KG) - iKG}{2\phi'(KG) + iKG}e^{2\phi(KG)/G}$$
$$= \frac{\sqrt{4-(KG)^2} - iKG}{\sqrt{4-(KG)^2} + iKG}e^{2\phi(KG)/G},$$

so that

$$\mathrm{Im}(\gamma) = -\frac{KG}{2}\sqrt{4-(KG)^2}\,e^{2\phi(KG)/G},$$

and the final equation is

$$\frac{\pi^3}{512}G\frac{dG}{d\tau} = \frac{\pi(\sigma-2)}{16\sigma}G + \sqrt{4-(KG)^2}KG\,e^{2\phi(KG)/G}. \tag{36}$$

H. Evaluation of the phase Φ

While we did not need to know the phase Φ in order to determine Eq. (23) for G, we do need to evaluate Φ if we are to compare the numerical solution v of (2) with the asymptotic expansion (7).

With template function $T = \delta(\xi - \xi_0)$ and choosing the constant $C = V_0(\xi_0)$, the pinning condition (4) is

$$\mathrm{Re}\left(e^{i\Phi(\tau)}e^{-iG(\tau)\xi_0^2/4}V_{\rm reg}\right) = V_0(\xi_0) + \text{T.S.T},$$

where T.S.T stands for transcendentally small terms in G (coming from $V_{\rm exp}$). Since $V_{\rm reg}$ is real this gives

$$\cos\left(\Phi - \frac{G\xi_0^2}{4}\right)V_{\rm reg}(\xi_0) = V_0(\xi_0). \tag{37}$$

Inserting the expansions (7) gives at leading order

$$-\frac{1}{2}\left(\Phi_0 - \frac{\xi_0^2}{4}\right)^2 V_0(\xi_0) + V_1(\xi_0) = 0,$$

so that

$$\Phi_0 = \frac{\xi_0^2}{4} \pm \sqrt{\frac{2V_1(\xi_0)}{V_0(\xi_0)}}.$$

With $\xi_0 = 2$ this gives $\Phi_0 \approx 2.1942$.

I. Initial transients

The analysis thus far assumes that G' and Φ' are exponentially small in G, giving a balance between the terms on the right-hand side of Eq. (21). However, for short times there may be an initial transient in which

$$-\Phi' V + \frac{G'\xi^2}{4}V$$

is not small compared to

$$\frac{G^2\xi^2 V}{4},$$

which affects the calculation of V_1, and therefore the left-hand side of (21).

If we include these terms in the correction to V_0 we find

$$V_{\rm reg} \sim V_0 + G^2V_1 + G'V_1 - \Phi'\tilde{V}_1 + \cdots,$$

where

$$\frac{\partial^2\tilde{V}_1}{\partial\xi^2} + 5V_0^4\tilde{V}_1 - \tilde{V}_1 = -V_0,$$

so that

$$\tilde{V}_1 = v_1\int_0^\xi \frac{v_2V_0\,d\bar{\xi}}{4} + v_2\int_\xi^\infty \frac{v_1V_0\,d\bar{\xi}}{4}$$
$$= -\frac{3^{1/4}(\cosh 2\xi - 2\xi\sinh 2\xi)}{4\cosh^{3/2}2\xi}.$$

In this case

$$\int_0^\infty V_{\rm reg}^2\,d\xi \sim \int_0^\infty V_0^2\,d\xi + 2(G^2+G')\int_0^\infty V_0V_1\,d\xi$$
$$- 2\Phi'\int_0^\infty V_0\tilde{V}_1\,d\xi + \cdots$$
$$\sim b_0 + 2(G^2+G')c_0 + \cdots,$$

since

$$\int_0^\infty V_0\tilde{V}_1\,d\xi = 0.$$

Thus Eq. (21) becomes, for $G > 0$,

$$c_0\left(2G\frac{dG}{d\tau} + \frac{d^2G}{d\tau^2}\right) = \frac{(d\sigma-2)b_0}{2\sigma}G - A_{d_c}^2e^{-\pi/G}. \tag{38}$$

A similar calculation can be performed for $G < 0$; combining the two results gives

$$c_0\left(2G\frac{dG}{d\tau} + \frac{d^2G}{d\tau^2}\right) = \frac{(d\sigma - 2)b_0}{2\sigma}G - A_{d_c}^2 \operatorname{sgn}(G)e^{-\pi/|G|}. \tag{39}$$

The behavior of (38) is easier to see by writing it as the first-order system

$$c_0\frac{d\beta}{d\tau} = \frac{(d\sigma - 2)b_0}{2\sigma}G - A_{d_c}^2 \operatorname{sgn}(G)e^{-\pi/|G|}, \tag{40}$$

$$\frac{dG}{d\tau} = \beta - G^2. \tag{41}$$

We see that this system is slow-fast: β evolves exponentially slowly by comparison to G. Thus there is an initial fast transient in which G evolves to lie on the slow manifold $\beta = G^2$, after which the slow dynamics of (21) take over.

In the critical case $d\sigma = 2$ the system of Eqs. (40) and (41) is similar to that derived in [18] at leading order. In [18] the exponential term is $e^{-\pi/\beta^{1/2}}$ rather than $e^{-\pi/|G|}$; however, during the fast dynamics right-hand side of (40) is negligible, while during the slow dynamics $\beta^{1/2}$ is exponentially close to $|G|$, so that asymptotically the systems are equivalent. In [18] higher-order terms in the coefficient c_0 are included (through a numerical fit rather than through an asymptotic expansion), but there is no corresponding attempt to calculate higher-order terms in the coefficient of the exponential.

J. Subcritical case

Equations (40) and (41) are also valid in the subcritical case $d\sigma < 2$. In that case the fast transient is not confined to the initial evolution but reappears periodically as the system performs an interesting relaxation oscillation, which we now describe.

With an initial condition $G = 0$, $\beta = \beta_0 > 0$, say, there is an initial fast transient in which $\beta = \beta_0$ is constant and G moves from zero to $\beta_0^{1/2}$ [which we suppose is $O(d\sigma - 2)$]. The system then follows the slow manifold $\beta = G^2$ with the dynamics given by (21). In the subcritical case there is no finite G solution, and G decreases slowly from $\beta_0^{1/2}$ to zero. However, at $G = 0$ the time derivative

$$\frac{dG}{d\tau} = \frac{(d\sigma - 2)b_0}{4\sigma c_0} < 0.$$

Thus G continues to negative values, with the dynamics still given by (21). For negative G the fast equation (41) is unstable, but because the solution became exponentially close to the slow manifold in the progression from $(\beta, G) \approx (\beta_0, \beta_0^{1/2})$ to $(\beta, G) \approx (0, 0)$, it takes a long time for the difference $\beta - G^2$ to grow sufficiently for the fast dynamics to take over. This happens when (β, G) reaches $(\beta_0, -\beta_0^{1/2})$, at which point there is a fast transition in which β is constant (and equal to β_0) and G varies quickly from $-\beta_0^{1/2}$ to $\beta_0^{1/2}$. Such behavior, in which the solution of a dynamical system follows an unstable manifold for a significant time, is often known as a canard [46,47], and it follows in this case from the invariance of (40) and (41) under $\tau \to -\tau$, $G \to -G$. Once the solution reaches the slow manifold again at $(\beta, G) \approx (\beta_0, \beta_0^{1/2})$ the cycle repeats. We show an example of the phase plane,

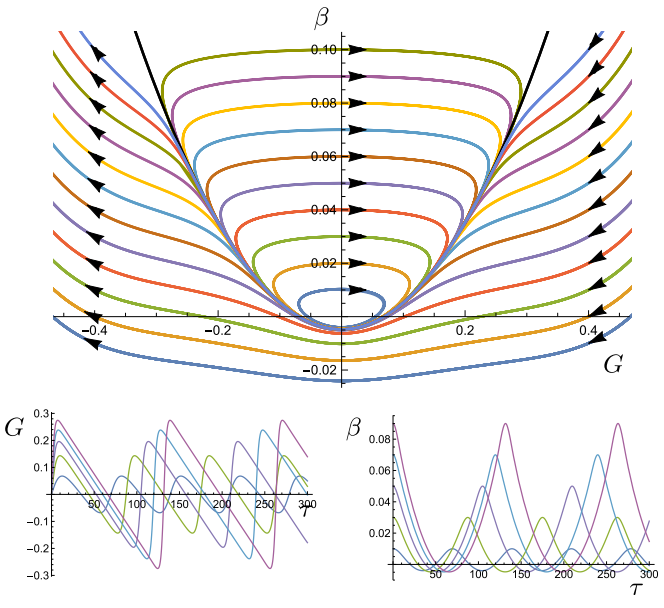

FIG. 2. Top panel: Phase plane for (40) and (41) when $(d\sigma - 2)b_0/2\sigma = 0.001$. Bottom panels: $G(\tau)$ and $\beta(\tau)$ when $(d\sigma - 2)b_0/2\sigma = 0.001$, for initial conditions $G = 0$ and $\beta = 0.1, 0.3, 0.5, 0.7, 0.9$.

Eqs. (40) and (41), and some sample trajectories, in Fig. 2. Nevertheless, a more systematic study of the relevant subcritical phenomenology at the PDE level is a topic of substantial interest in in its own right that is worthwhile to be considered in future work.

On a finite domain there is the extra complication that the turning point at $\xi = 2/|G|$ is forced to exit the domain for a range of values of G close to zero, with the slow dynamics for this range given by (36) rather than (34). However, when G is very close to zero, the exponential terms in these equations are insignificant in comparison to the term proportional to $d\sigma - 2$, so in fact this change makes very little difference.

III. NUMERICAL VERIFICATION

Equation (21) predicts the existence of a stable branch of solutions bifurcating from $d\sigma = 2$. We compare this prediction with direct numerical simulations of (2) by fixing $d = 1$ (for which the ground-state soliton is analytically available) and varying σ close to $\sigma_c = 2$ although, as indicated above, our results can be straightforwardly applied to the radial, higher-dimensional case. The relevant bifurcation diagram can be seen in Fig. 1. Here we compare the PDE results obtained directly from Eq. (2) with the normal form of Eq. (21), finding excellent agreement between the two. This is shown in Fig. 3. The top panel showcases the exponential nature of the relevant bifurcation over *eight orders of magnitude* of the associated ODE [i.e., the positive steady state of Eq. (21)] and PDE data, in excellent agreement between the two. Notice that the finite nature of the computation leads to some nearly imperceptible oscillations in the top panel of the figure, also observed but not commented earlier [30,32]. The full power of our methodology is revealed when factoring out the

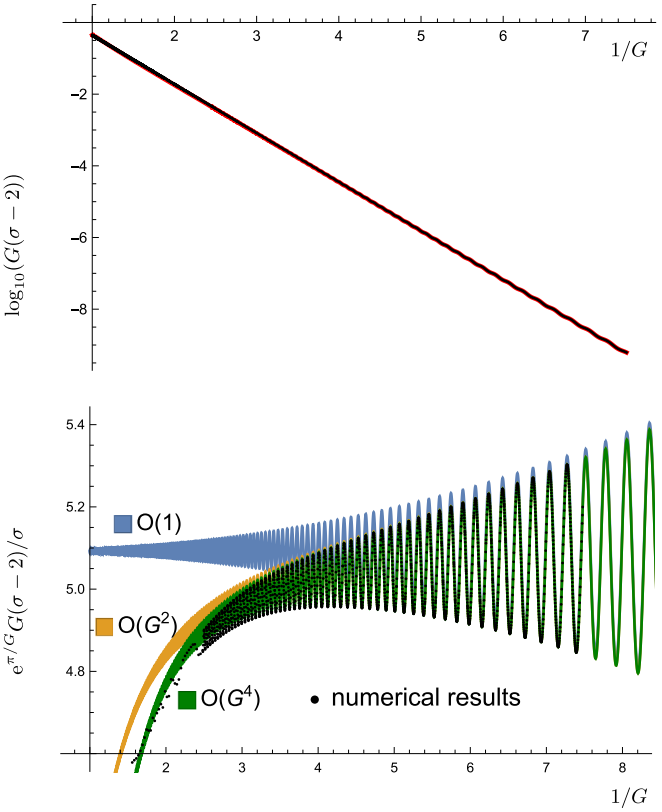

FIG. 3. Collapsing solution branch for $d = 1$, domain size $K = 50$. Top panel: The leading-order asymptotic solution (black) is shown against a stationary numerical solution of (2) (red). The two lines essentially coincide. The weak deviations from linearity are due to the sinusoidal term in (35). Bottom panel: *Exponentially scaled* illustration of the same result to show the accuracy of our higher-order analysis, in which the expansion of a and b in (23) is truncated at leading order, at $O(G^2)$ and at $O(G^4)$. The full numerical result calculated using CHEBFUN [41] is shown in black.

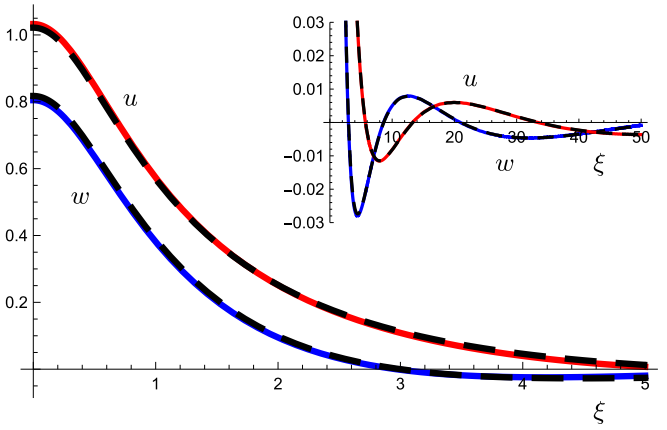

FIG. 4. Comparison of the numerical (black, dashed) and asymptotic approximations of the steady solution $v = u + iw$ of (2) when $K = 50$, $\sigma = 2.001$. The main plot shows the near field, where the asymptotic solution is given by (7) truncated at $O(G^2)$; the inset shows a uniform approximation to the far field combining (17) and (14), truncated at leading order, the details of which are given in (A1).

exponentially small leading order by rescaling through $e^{\pi/G}$; see the bottom panel of Fig. 3. Here we present the first- and second-order corrections, illustrating how they progressively match, in a remarkably *quantitative* fashion, the PDE results.

In Fig. 4 we show how we capture not only the rate of collapse but also near perfectly both the real and the imaginary parts of the profile of the associated solution $u + iw$. The asymptotic profile in the far field is a uniform approximation, the details of which are presented in the Appendix.

Lastly, our methodology also enables an excellent capturing of the associated dynamics as shown in Fig. 5. The initial condition for the numerical solution is the analytical expression of the ground-state soliton for $d = 1$: $v(\xi, \tau = 0) = 3^{1/4}\sqrt{\mathrm{sech}2\xi}$, the initial condition for the blowup rate is $G(\tau = 0) = 0$. Here, in addition to the spatiotemporal evolution of the field in the (ξ, τ) variables, the evolution of the collapse rate $G(\tau)$ towards its stable asymptotic value is observed in the inset and compared against the numerical solution, showing excellent agreement. We have found this to be true for generic localized initial conditions in the vicinity of the unstable solitary wave solution.

IV. CONCLUSIONS AND FUTURE CHALLENGES

We have revisited the collapse of a nonlinear Schrödinger equation. A unifying, mathematically compact, yet quantitatively accurate normal form is identified that combines the famous log-log behavior at the critical point, the emergence of a stable self-similarly collapsing branch past that point, the exponentially small breaking of the pseudoconformal invariance of the critical point, the Hamiltonian nature of the original model, and the dissipative features of the

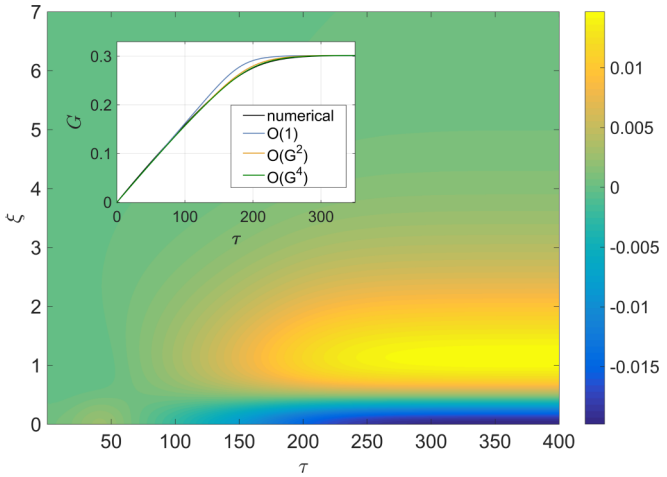

FIG. 5. $K = 50$, $\sigma = 2.001$. Spatiotemporal evolution ($\xi - \tau$ space) of $|v|^2 - |V_0|^2$. The inset shows the evolution of $G(\tau)$ for the full numerical solution of (2) (black), and for the solution of the finite domain version of (23) truncated at $O(1)$ (blue), $O(G^2)$ (orange), and $O(G^4)$ (green). The renormalized NLS reaches a steady-state solution after $\tau \approx 300$.

renormalized dynamics. This constitutes a broadly applicable (in optics, BECs, and beyond) normal form associated with the onset of collapse. This also prompts numerous exciting questions for the future, such as, e.g., on the stability of the collapsing solutions or on the potential normal form for generalized Korteweg–de Vries equations [48,49] and their traveling waves, of broad relevance to water waves and plasmas.

APPENDIX: UNIFORM APPROXIMATION IN THE FAR FIELD

In the far field we found in Sec. II G the "outer" approximation, away from the turning point, as

$$V_{\rm reg} \sim \alpha G^k e^{i\phi_2(\rho)/G} B_0(\rho) + \beta G^k e^{-i\phi_2(\rho)/G} B_0(\rho) \quad \rho > 2,$$
$$V_{\rm reg} \sim G^k e^{\phi(\rho)/G} A_0(\rho) + \gamma G^k e^{-\phi(\rho)/G} A_0(\rho) \quad \rho < 2,$$

and the "inner" approximation, near the turning point, as

$$V_{\rm reg} \sim a_0\sqrt{\pi}\, G^{k-1/6}[\lambda {\rm Ai}(-s) + \mu {\rm Bi}(-s)],$$

with $\rho = 2 + G^{2/3}s$. In order to compare with the numerical solution, it is helpful to have a uniformly valid asymptotic approximation. If we set

$$X(\rho) = \left(\frac{3\phi_2(\rho)}{2G}\right)^{2/3} = \left[\frac{3}{2G}\int_2^\rho \left(\frac{\bar\rho^2}{4} - 1\right)^{1/2} d\bar\rho\right]^{2/3}$$

for $\rho > 2$ and

$$X(\rho) = -\left(\frac{3(\phi(2) - \phi(\rho))}{2G}\right)^{2/3} = -\left[\frac{3}{2G}\int_\rho^2 \left(1 - \frac{\bar\rho^2}{4}\right)^{1/2} d\bar\rho\right]^{2/3}$$

for $\rho < 2$, then

$$V_{\rm uniform}(\rho) = a_0 2^{1/2}\sqrt{\pi} G^k \lambda \left(\frac{X(\rho)}{\rho^2 - 4}\right)^{1/4} {\rm Ai}(-X(\rho)) + a_0 2^{1/2}\sqrt{\pi} G^k \mu \left(\frac{X(\rho)}{\rho^2 - 4}\right)^{1/4} {\rm Bi}(-X(\rho)) \tag{A1}$$

is a uniformly valid, leading-order approximation for all $\rho > 0$. The inset in Fig. 4 shows $V_{\rm uniform}(G\xi)e^{iG(\Phi_0 - i\xi^2/4)}$.

[1] M. J. Ablowitz and P. A. Clarkson, *Solitons, Nonlinear Evolution Equations and Inverse Scattering* (Cambridge University Press, Cambridge, England, 1991).
[2] M. J. Ablowitz, B. Prinari, and A. D. Trubatch, *Discrete and Continuous Nonlinear Schrödinger Systems* (Cambridge University Press, Cambridge, England, 2004).
[3] C. Sulem and P. L. Sulem, *The Nonlinear Schrödinger Equation* (Springer-Verlag, New York, 1999).
[4] P. G. Kevrekidis, D. J. Frantzeskakis, and R. Carretero-González, *The Defocusing Nonlinear Schrödinger Equation: From Dark Solitons and Vortices to Vortex Rings* (SIAM, Philadelphia, 2015).
[5] E. Infeld and G. Rowlands, *Nonlinear Waves, Solitons and Chaos* (Cambridge University Press, Cambridge, England, 1990).
[6] M. J. Ablowitz, *Nonlinear Dispersive Waves: Asymptotic Analysis and Solitons* (Cambridge University Press, Cambridge, England, 2011).
[7] Th. Dauxois and M. Peyrard, *Physics of Solitons* (Cambridge University Press, Cambridge, England, 2006).
[8] A. Hasegawa, *Solitons in Optical Communications* (Clarendon Press, Oxford, England, 1995).
[9] Yu. S. Kivshar and G. P. Agrawal, *Optical Solitons: From Fibers to Photonic Crystals* (Academic Press, San Diego, CA, 2003).
[10] M. Kono and M. M. Skorić, *Nonlinear Physics of Plasmas* (Springer-Verlag, Heidelberg, 2010).
[11] L. P. Pitaevskii and S. Stringari, *Bose-Einstein Condensation* (Oxford University Press, Oxford, England, 2003).
[12] C. J. Pethick and H. Smith, *Bose-Einstein Condensation in Dilute Gases* (Cambridge University Press, Cambridge, England, 2002).
[13] G. Fibich, *The Nonlinear Schrödinger Equation, Singular Solutions and Optical Collapse* (Springer-Verlag, New York, 2015).
[14] R. W. Boyd, S. G. Lukishova, and Y. R. Shen, *Self-Focusing: Past and Present* (Springer-Verlag, New York, 2009).
[15] G. Fibich and G. Papanicolaou, SIAM J. Appl. Math. **60**, 183 (1999).
[16] L. Bergé, Phys. Rep. **303**, 259 (1998).
[17] Yu. S. Kivshar and D. E. Pelinovsky, Phys. Rep. **331**, 117 (2000).
[18] P. M. Lushnikov, S. A. Dyachenko, and N. Vladimirova, Phys. Rev. A **88**, 013845 (2013).
[19] P. M. Lushnikov and N. Vladimirova, Opt. Express **23**, 31120 (2015).
[20] B. Shim, S. E. Schrauth, A. L. Gaeta, M. Klein, and G. Fibich, Phys. Rev. Lett. **108**, 043902 (2012).
[21] H. Koch, Nonlinearity **28**, 545 (2015).
[22] K. Yang, S. Roudenko, and Y. Zhao, Nonlinearity **31**, 4354 (2018).
[23] P. M. Lushnikov, Phys. Lett. A **374**, 1678 (2010).
[24] K. D. Moll, A. L. Gaeta, and G. Fibich, Phys. Rev. Lett. **90**, 203902 (2003).
[25] L. T. Vuong, T. D. Grow, A. Ishaaya, A. L. Gaeta, G. W.'t Hooft, E. R. Eliel, and G. Fibich, Phys. Rev. Lett. **96**, 133901 (2006).
[26] A. Sagiv, A. Ditkowski, and G. Fibich, Opt. Express **25**, 24387 (2017).
[27] C.-A. Chen and C.-L. Hung, Phys. Rev. Lett. **125**, 250401 (2020).
[28] E. A. Donley, N. R. Claussen, S. L. Cornish, J. L. Roberts, E. A. Cornell, and C. E. Wieman, Nature (London) **412**, 295 (2001).
[29] S. L. Cornish, S. T. Thompson, and C. E. Wieman, Phys. Rev. Lett. **96**, 170401 (2006).
[30] M. J. Landman, G. C. Papanicolaou, C. Sulem, and P. L. Sulem, Phys. Rev. A **38**, 3837 (1988).
[31] B. J. LeMesurier, G. Papanicolaou, C. Sulem, and P. L. Sulem, Physica D **31**, 78 (1988).

[32] C. I. Siettos, I. G. Kevrekidis, and P. G. Kevrekidis, Nonlinearity **16**, 497 (2003).
[33] T. Zibold, E. Nicklas, and C. Gross, and M. K. Oberthaler, Phys. Rev. Lett. **105**, 204101 (2010).
[34] F. Merle, P. Raphaël, and J. Szeftel, Geom. Funct. Anal. **20**, 1028 (2010).
[35] P. M. Lushnikov, Pis'ma Zh. Theo. Fiz. **62**, 461 (1995) [JETP Lett. **62**, 461 (1995)].
[36] J. Holmer, R. Platte, and S. Roudenko, Nonlinearity **23**, 977 (2010).
[37] M. Landman, G. Papanicolaou, C. Sulem, P. Sulem, and X. Wang, Physica D **47**, 393 (1991).
[38] G. Fibich, N. Gavish, and X.-P. Wang, Physica D **211**, 193 (2005).
[39] G. Fibich and N. Gavish, Physica D **237**, 2696 (2008).
[40] The specific choice (among numerous possible choices) does not affect the normal form obtained.
[41] *Chebfun Guide*, edited by T. A. Driscoll, N. Hale, and L. N. Trefethen (Pafnuty Publications, Oxford, 2014).
[42] C. M. Bender and S. A. Orszag, *Advanced Mathematical Methods for Scientists and Engineers* (Springer-Verlag, New York, 1999).
[43] J. P. Boyd, Acta Appl. **56**, 1 (1999).
[44] G. Fibich and A. L. Gaeta, Opt. Lett. **25**, 335 (2000).
[45] G. Fibich and F. Merle, Physica D **155**, 132 (2001).
[46] E. Benoît, J. F. Callot, F. Diener, and M. Diener, Collect. Math. **32**, 37 (1981).
[47] W. Eckhaus, Relaxation oscillations including a standard chase on French ducks, in *Asymptotic Analysis II*, edited by F. Verhulst, Lecture Notes in Mathematics, Vol. 985 (Springer, Berlin, Heidelberg, 1983).
[48] J. L. Bona, V. A. Dougalis, O. A. Karakashian, and W. R. McKinney, J. Comput. Appl. Math. **74**, 127 (1996).
[49] P. Amodio, C. J. Budd, O. Koch, V. Rottscäfer, G. Settanni, and E. Weinmüller, Physica D **401**, 132179 (2020).